RESEARCH ARTICLE | JANUARY 19 2023

Small-tilt measurement based on weak-value-amplification with balanced homodyne detection

Special Collection: MXenes - Physics and Devices

ChaoXia Zhang ; YongLang Lai ; RongGuo Yang ; Kui Liu ; Jing Zhang ; HengXin Sun ;
JiangRui Gao

Appl. Phys. Lett. 122, 031107 (2023)
https://doi.org/10.1063/5.0132992

Small-tilt measurement based on weak-value-amplification with balanced homodyne detection

Cite as: Appl. Phys. Lett. **122**, 031107 (2023); doi: 10.1063/5.0132992
Submitted: 1 November 2022 · Accepted: 5 January 2023 ·
Published Online: 19 January 2023

ChaoXia Zhang,[1,2] YongLang Lai,[1,2] RongGuo Yang,[1,2,3,a)] Kui Liu,[1,2,3] Jing Zhang,[1,2,3] HengXin Sun,[1,2,3] and JiangRui Gao[1,2,3]

AFFILIATIONS

[1]College of Physics and Electronic Engineering, Shanxi University, Taiyuan 030006, People's Republic of China
[2]State Key Laboratory of Quantum Optics and Quantum Optics Devices, Taiyuan 030006, People's Republic of China
[3]Collaborative Innovation Center of Extreme Optics, Shanxi University, Taiyuan 030006, People's Republic of China

Note: This paper is part of the APL Special Collection on MXenes - Physics and Devices.
[a)]**Author to whom correspondence should be addressed:** yrg@sxu.edu.cn

ABSTRACT

We experimentally realize a great precision enhancement in the small-tilt measurement by using a Sagnac interferometer and balanced homodyne detection (BHD) of high-order optical modes, together with the weak-value amplification (WVA) technique. Smaller minimum measurable tilt and higher signal-to-noise ratio can be obtained by using BHD, compared with the split detection. The precision of 3.8 nrad can be obtained under our present experimental condition. It is shown that combining WVA technique and BHD can strengthen each other's advantages and can behave better for some special application scenarios, such as extremely weak output, wider measurement bandwidth, etc. Moreover, the precision can be further enhanced by experimental parameter optimization.

Quantum measurement is not only an important tool to explore the micro-world but also a key to the interpretation of quantum mechanics and the application of quantum information. For a long time, the improvement of precision measurement technology and the breakthrough of higher measurement precision are the goals that people strive to pursue. As one of the basic facets in precision measurement, optical tilt and displacement measurement have attracted more attention in recent years, which has been applied in many fields, such as biological measurement,[1] atomic force microscopy,[2] high-resolution quantum imaging,[3–5] and gravitational wave detection.[6,7]

On the one hand, optimizing the probe state is an effective way to improve the precision of quantum measurement. Consider about the small-displacement[8–16] and small-tilt[12] measurement, high-order-mode light or spatial squeezed light is often utilized as the probe state, due to their spatial transverse property. However, the technical difficulty of preparing these probe states is usually large. Therefore, to find a convenient alternative to optimize the probe state, the weak-value amplification (WVA) technique, which has an optimized probe state that contains a weak value, is under our consideration. The weak-value amplification (WVA) technique, which was first proposed by Aharanov *et al.* in 1988[17] and widely used in many different systems, has been proved to have its advantages for precision enhancement not only theoretically[18–20] but also experimentally.[21–28] Due to the preselection and post-selection states of the system, WVA can take larger complex values beyond the eigenvalues of the observed quantities, resulting in abnormal amplification of small physical quantities.[22–26] For example, the interferometric WVA technique was used to amplify very small transverse deflections of an optical beam, and WVA factors of over 100 are achieved.[22] WVA in the azimuthal degree of freedom was demonstrated, and a sensitive estimation of angular rotation of the spatial-mode light with the corresponding effective amplification factors as large as 100 was got.[24] Moreover, the precision enhancement of weak-value-based metrology together with the power-recycling technique[25,27,28] and the almost-balanced weak-value amplification technique[29,30] were investigated. Two almost-balanced (almost same intensity) output beams are post-selected and injected into the balanced detectors in almost-balanced weak-value amplification technique. While for WVA technique, a strong and a weak output beam (from constructive and destructive interference) are post-selected, and only the weak beam from the dark port of the interferometer is utilized in the detection system, which means that effective beam tilt information can be obtained by post-selecting only extremely small part of those tilted photons.

On the other hand, optimizing the detection system is also of great importance. The balanced homodyne detection (BHD), which usually consists of a pair of ETX-500 photodiodes (detection bandwidth: 140 MHz, dark current: 12 nA, and NEP: 125 nW), allows us to place different carriers in the spectrum and to detect very weak signals and can also be used in squeezed/entangled light observation, optical homodyne tomography, etc., to get the quantum noise. With the development of the research of laser spatial characteristics, it was also applied to measure the spatial information of light beam,[10–16] such as the displacement and the tilt. It is shown that the TEM_{10} homodyning scheme outperforms split detection (SD) for all values of squeezing although the quantum noise limit of displacement measurement can be surpassed by using squeezed light of appropriate spatial modes for both schemes,[15] and it is proved that the standard SD is only 64% efficient relative to the TEM_{10} homodyne detection.[16]

In this Letter, we demonstrate the precision enhancement in an optical small-tilt measurement applying the WVA + BHD technique both theoretically and experimentally. The combination of WVA and BHD techniques based on the high-order mode brings a better performance to detect extremely weak signal with fast detection speed and large frequency bandwidth.

Assume that the probe state is the Hermite–Gauss (HG) fundamental (TEM_{00}) mode denoted by $\psi_0(x)$, which is tilted at the waist spot with tilt quantity θ. It is equivalent to adding a transverse momentum, $k = 2\pi \sin\theta/\lambda$, and then the probe state after the tilt is represented by $\psi_0^\theta(x)$. In the case of small tilt, we can consider the Taylor expand of the tilted probe state only the first order,[16]

$$\psi_0^\theta(x) = \exp(ikx)\psi_0(x) \approx (1 + ikx)\psi_0(x)\,. \tag{1}$$

By using the relation between TEM_{00} and TEM_{10} modes $\psi_0(x) = \omega_0\psi_1(x)/2x$, the above equation can be changed into

$$\psi_0^\theta(x) \approx \psi_0(x) + \frac{i\omega_0 k}{2}\psi_1(x)\,. \tag{2}$$

Here, $\psi_0(x)$ is the TEM_{00} mode and $\psi_1(x)$ is the TEM_{10} mode. Thus, the TEM_{10} mode can be induced by the tilt of the fundamental TEM_{00} mode, and the induced TEM_{10} mode is proportional to the tilt signal. Then, the tilt information can be measured by using the BHD.[10–12,14–16]

The schematic diagram of measuring small tilt with BHD using and not using WVA technique is shown in Figs. 1(a) and 1(b), respectively. Here, the mode order of the signal (tilt) beam and the local beam is not the same, which is different from that measuring the quadrature components. The Sagnac interferometer containing the tilt modulation system (TMS), which is introduced into the signal field, is the main part of the weak-value measurement system. The weak-value measurement operation involves two quantum states: the system and the pointer. The path information of Sagnac interferometer is called the system, expressed by $|+\rangle$ for clockwise path and $|-\rangle$ for counterclockwise path.[31] We refer to the beam's transverse amplitude distributions as the pointer, described by $|\psi_i\rangle$. A standard weak measurement process consists of three steps: preselection, weak interaction, and post-selection. Preselection couples the initial state of the system $|i\rangle$ and the pointer $|\psi_i\rangle$ in the product state $|i\rangle|\psi_i\rangle$. Weak interaction produces entanglement between the system and the pointer states, and the interaction Hamiltonian is

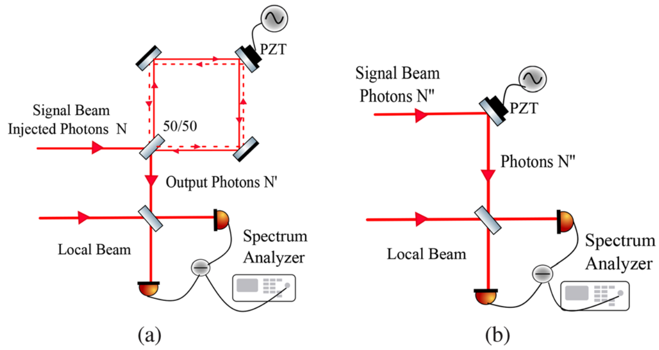

FIG. 1. BHD system of weak-value measurement (a) and conventional measurement (b). PZT: piezoelectric transducers.

$$H_{\rm int} = g(t)\hat{A}k\hat{x}, \tag{3}$$

where $g(t)$ is the normalized parameter that varies with time. $\hat{A} = |+\rangle\langle+| - |-\rangle\langle-|$ is the operator of the system state. k is the transverse momentum kick of light beam induced by the mirror vibration, and $\hat{x}$ is the operator of the pointer state. Post-selection process is the projection of the entangled state onto the final state $|f\rangle$ of the system. The final state is

$$\begin{aligned}|\psi_f\rangle &= \langle f|\hat{U}|i\rangle|\psi_i\rangle/\sqrt{P}\\ &= \langle f|\exp\left(-i\int H_{\rm int}dt|i\rangle|\psi_i\rangle/\sqrt{P}\right.\\ &\approx \langle f|(1 - i\hat{A}k\hat{x}|i\rangle|\psi_i\rangle/\sqrt{P}\\ &= \langle f|i\rangle(1 - iA_w k\hat{x}|\psi_i\rangle/\sqrt{P} = |\psi_i(x - A_w k)\rangle,\end{aligned} \tag{4}$$

where $A_w = \frac{\langle f|A|i\rangle}{\langle f|i\rangle}$ is the weak value. $P = |\langle f|i\rangle|^2$ is the post-selection probability with initial state $|i\rangle = \frac{1}{\sqrt{2}}(e^{-i\phi/2}|+\rangle + e^{i\phi/2}|-\rangle)$ and final state $|f\rangle = \frac{1}{\sqrt{2}}(|+\rangle - |-\rangle)$, where ϕ is the relative phase between the clockwise and the counterclockwise paths of the Sagnac interferometer.[31] ψ_i denotes the transverse amplitude distribution of one-dimensional Hermite–Gauss (HG) modes. One can see that there exists a transverse change of the beam, given by $A_w k$. The smaller the relative phase ϕ, the weaker the dark port beam, which results in a larger A_w, and then an amplified transverse change is $A_w k$.

A small transverse change $A_w k$ of a TEM_{00} mode can induce many higher order modes, and then the pointer state in one dimension has the following form:

$$\begin{aligned}\psi_i(x - A_w k) &\approx \psi_0(x) - i\frac{\omega_0 A_w k}{2}\psi_1(x)\\ &= \psi_0(x) - i\frac{\pi\omega_0 A_w \theta}{\lambda}\psi_1(x),\end{aligned} \tag{5}$$

$$\psi_n(x) = \left(\frac{2}{\pi\omega_0}\right)^{1/4}\frac{1}{\sqrt{n!2^n}}H_n\left(\frac{\sqrt{2}x}{\omega_0}\right)e^{\frac{-x^2}{\omega_0^2}}, \quad n = 0, 1, \ldots, \tag{6}$$

where ω_0 is the waist of the TEM_{00} mode and $H_n(x)$ is the Hermite polynomial with n representing the order of the HG mode. Obviously, TEM_{10} induced by the translation of TEM_{00} contains the tilt information, which can be extracted by using the TEM_{10} mode as the local beam.

In the BHD system, the photon number difference $\hat{N}_{-}^{BHD}$ between two detectors is proportional to the difference of photocurrent,[15] and thus, we obtain

$$\hat{N}_{-}^{BHD} = \sqrt{N_{LO}}\left(2\sqrt{N'}A_w k\omega_0 + \delta\hat{X}_S^{-}\right), \tag{7}$$

where the first term is the signal part including the small-tilt information and the second term is the quantum noise. N' and N_{LO} are the mean photon numbers of the signal and local beams, respectively. $\delta\hat{X}_s^{-} = (\delta\hat{a} - \delta\hat{a}^{\dagger})/i$ is the quadrature phase fluctuation of the TEM_{10} mode included in signal light, where $\hat{a}$ and $\hat{a}^{\dagger}$ are the corresponding annihilation and creation operator, respectively.

Then, the signal-to-noise ratio (SNR) of the tilt measurement applying the BHD system is

$$SNR_{BHD} = \left(\frac{2\sqrt{N'}A_w k\omega_0}{\delta\hat{X}_S^{-}}\right)^2, \tag{8}$$

where $\delta X_s^{-} = \sqrt{\langle\delta^2\hat{X}_s^{-}\rangle}$. Consider that $N' = N|\langle f|i\rangle|^2$ in which N is the number of photons injected into Sagnac interferometer (bright port). Then, N' can also be regarded as the number of photons output from the dark port of the Sagnac interferometer and can be detected by the BHD system. For coherent light ($\delta\hat{X}_s^{-} = 1$), the corresponding SNR can be defined as

$$SNR_{BHD} = \left(2\sqrt{N|\langle f|i\rangle|^2}A_w k\omega_0\right)^2 = \left(2\sqrt{N}\cos\frac{\phi}{2}k\omega_0\right)^2. \tag{9}$$

The minimum measurable tilt can be generally defined by the tilt with $SNR = 1$, which is given by

$$\theta_{\min}^{BHD} = \frac{\lambda}{4\pi\omega_0\sqrt{N}\cos\frac{\phi}{2}}. \tag{10}$$

As is known, the SNR and the minimum measurable values are related to the measurement precision. The higher the SNR or the smaller the minimum measurable value, the higher the measurement precision. The initial and final states of the system tend to be orthogonal when the relative phase ϕ is small enough; meanwhile, the SNR becomes higher and the minimum measurable value becomes smaller with the same waist and photon number. When $\phi = 0$, the expression of the minimum measurable tilt corresponds to the standard quantum limit. It is worth to mention that destructive interference is the essence of the WVA process. However, at the dark port, destructive interference only happens to the TEM_{00} mode and simultaneously constructive interference to the TEM_{10} mode without any loss of the tilt information. In this sense, the post-selection process is not simply a background filtering process but a destructive interference process.

In addition, the split detection (SD) is also a commonly used way in small-displacement/tilt measurement. When the beam is initially centered on the detector, the mean value of the photocurrent difference is proportional to the relative displacement of the beam with respect to the detector center.[9,16] The SNR and the minimum measurable tilt detected by SD can be obtained as

$$SNR_{SD} = \frac{2}{\pi}\left(2\sqrt{N}\cos\frac{\phi}{2}k\omega_0\right)^2, \tag{11}$$

$$\theta_{\min}^{SD} = \sqrt{\frac{\pi}{2}}\frac{\lambda}{4\pi\omega_0\sqrt{N}\cos\frac{\phi}{2}}. \tag{12}$$

As is shown in Fig. 2, under the same conditions, the "WVA + BHD" scheme results in higher SNR and smaller minimum measurable tilt, compared with the "WVA + SD" scheme. The SNR of using BHD has an improvement of 57% than that of using SD, due to a factor of $2/\pi$, according to Eqs. (9) and (11). The $2/\pi$ factor arises from the imperfect overlap between the fundamental mode being tilted (induced TEM_{10} mode included) and the equivalent zeroth flip mode of SD, since there is a π-phase flip at the center of SD.[15,16]

The experimental setup is shown in Fig. 3. A continuous wave solid-state YAG laser operating at 1064 nm is used to drive the system. The laser beam can be divided into two beams. One beam passing through the mode-conversion cavity MC2 is called the local beam, while the other beam passing through the mode-cleaner cavity MC1 is the signal beam, which next enters the weak-value measurement system and is tuned by the tilt modulation system. After that, the local and signal beams are coupled into the BHD system, and the BHD output can be analyzed by an electronic spectrum analyzer (ESA).

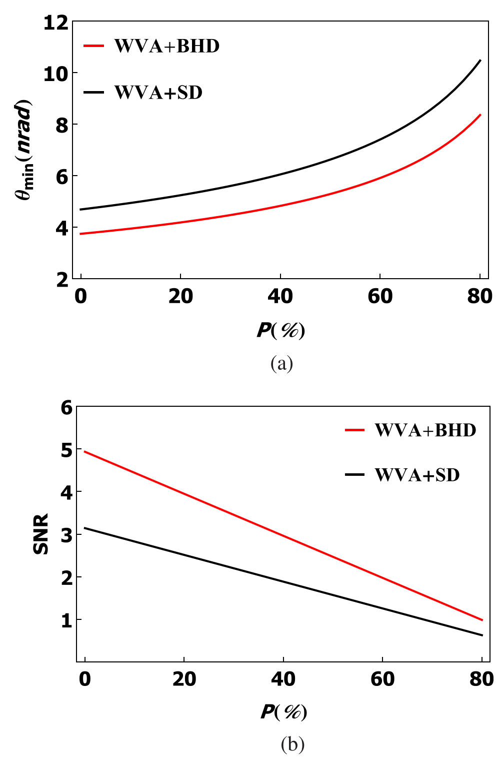

FIG. 2. (a) The minimum measurable tilt (a) and the SNR (b) vs the post-selection probability. $N = 5.352\,65 \times 10^{11}$, $\omega_0 = 60\,\mu$m.

Appl. Phys. Lett. 122, 031107 (2023); doi: 10.1063/5.0132992

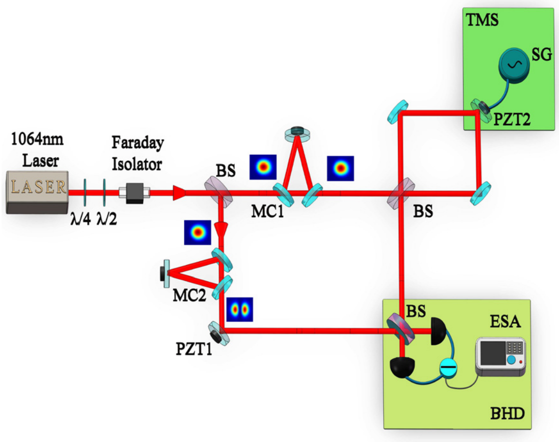

FIG. 3. Experimental setup. MC1: mode cleaner, MC2: mode converters, TMS: tilt modulation system, PZT1 and PZT2: piezoelectric transducers, SG: signal generator, BS: 50/50 beam splitter, BHD: balanced homodyne detection, ESA: electronic spectrum analyzer.

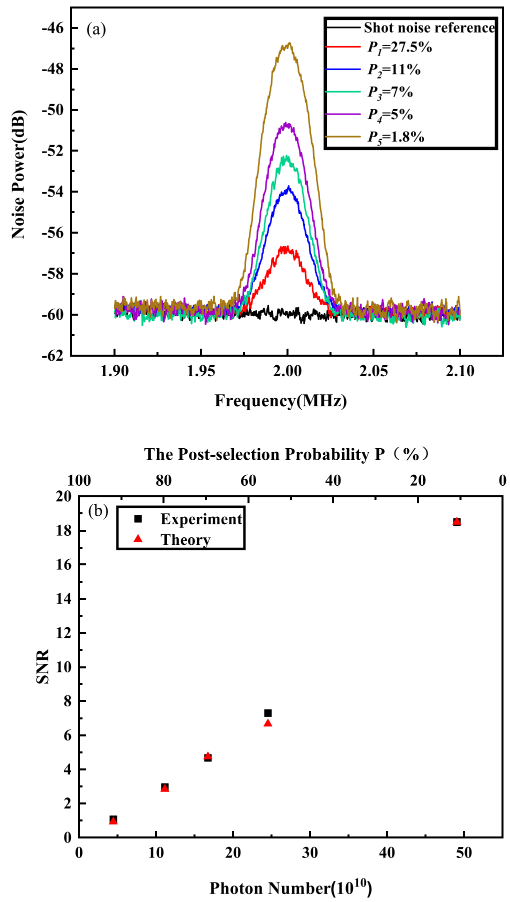

FIG. 4. (a) Noise power spectrum with different post-selection probabilities. (b) SNR vs the injected photon numbers of the Sagnac interferometer/the post-selection probability.

The input and output ports of the Sagnac interferometer are corresponding to the preselection and post-selection steps, respectively. While the weak interaction is from the tilt modulation system, the tilt modulation system consists of a mirror mounted on a piezoelectric transducer (PZT2) and a connected signal generator (SG). PZT2 is driven by a sine wave signal with a mechanical resonance frequency of 2 MHz. The experimental parameters are as follows: TEM_{00} waist $\omega_0 = 60\,\mu$m, the local beam power $P_{local} = 1$ mW, the resolution bandwidth $RBW = 24$ kHz, video bandwidth $VBW = 130$ Hz, and analyzing frequency $f = 2$ MHz.

According to Eq. (9), the relationship between SNR and the input photon number N, also the post-selection probability P of the interferometer, is investigated experimentally under different conditions. The phase ϕ is related to the post-selection probability P, and P is the ratio of the output power P_{out} to the input power P_{in}, i.e., $P = |\langle f|i\rangle|^2 = \sin^2\frac{\phi}{2} = P_{out}/P_{in}$. The photon number is proportional to the power, i.e., $N = \frac{P_{in}\cdot\lambda}{\hbar c\cdot RBW}$ and $N' = \frac{P_{out}\cdot\lambda}{\hbar c\cdot RBW}$.

The noise power spectrum under different post-selection probabilities is shown in Fig. 4(a), the output power of the weak-value measurement system is fixed at 55 μW, and the injected optical power is chosen to be 200 μW, 500 μW, 800 μW, 1.1 mW, and 3.2 mW. The SNR value in Fig. 4(b) is obtained according to $p = 10\log(SNR + 1)$, where p is the noise power spectrum [normalized to shot noise limit (SNL)]. In Fig. 4(b), the tilt corresponding to the maximum SNR is regarded as a reference value; based on which, the theoretical values of other points (represented by red triangles) can be derived. It is obvious that the signal beam power detected by the BHD is much smaller than the local beam power. During this process, the piezo driving voltage of the tilt modulation system remains unchanged. As is shown in Fig. 4(a), the smaller the post-selection probability, the larger the noise power. Here, the amplified signal measured by our system only depends on the injected beam power of the Sagnac interferometer. As is shown in Fig. 4(b), the lower the post-selection probability, the higher the SNR. Here, the amplified signal measured by our system only depends on the injected photon number N of the Sagnac interferometer, which means that effective beam tilt information can be obtained by post-selecting only extremely small part of those tilted photons. For comparison, the SNR of the conventional BHD system [Fig. 1(b)] is related to the photon number N'' detected from the BHD system. Obviously, in the conventional BHD system, N'' is usually very small due to the power limitation of the local beam and the saturation of the detector. Here, the WVA + BHD system is more convenient to get higher SNR than our previous "high-order-mode + BHD" system because increasing photon number is easier than increasing the order of the high-order modes.

Here, in Fig. 4, the output optical power P_{out} of the weak-value measurement system is kept a constant, and the results are obtained by changing the injected optical power P_{in}. Then, in Fig. 5, from another perspective, the injected optical power P_{in} is kept unchanged by changing the output optical power P_{out}. The injected beam power of the Sagnac interferometer is fixed at 70 μW, and the output beam power is tuned to be 55 μW, 35 μW, 11 μW, and 4 μW. The piezo driving voltage of the tilt modulation system still remains unchanged. Here, a low injected beam power is chosen, for better investigating the

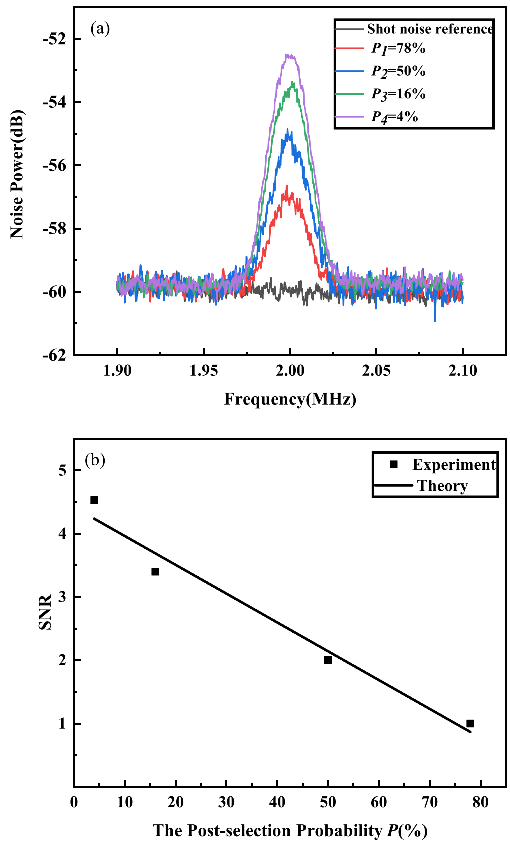

FIG. 5. Noise power spectrum (a) and the SNR (b) vs the post-selection probability (the solid line is the theoretical fitting curve).

influence of changing the dark port (from dark to bright) on the measurement results. It is important to note that the local beam power should still be much greater than the signal beam power when the dark port becomes bright. As is shown in Fig. 5, the smaller the post-selection probability, the larger the SNR. With the same injected power of the Sagnac interferometer, the weaker the dark port, the smaller the post-selection probability, the more the tilt information contained.

Generally, direct detection is hard to treat extremely weak photon number, due to the requirement for both high electronic gain and low noise of detector. However, our BHD system can avoid this shortcoming because of the existence of the local beam. BHD can work well even when the intensity of the signal beam is small, as long as the intensity of the signal beam is smaller than that of the local beam.[32]

According to Eq. (10), the minimum measurable tilt varies with the input power P_{in}, which is shown in Table I and Fig. 6. The post-selection probability is kept to be the optimized state under present experimental conditions, that is, $P = \frac{P_{out}}{P_{in}} \approx 3.3\%$. In Table I, the driving voltage on PZT2 is changed to keep SNR = 1 (the minimum measurable tilt, 3 dB noise on the spectrometer) and the post-selection probability remains unchanged, for each measurement. $RBW = 10\,\text{kHz}$, for more convenient and precise. As is shown, when input and output power are 1000 and 33 μW, respectively, separately, the smallest minimum measurable tilt can be obtained: $\theta_{\min} = 3.8\,\text{nrad}$. It is clear that increasing

TABLE I. The relationship table among the input and output power, the piezo driving voltage, and the minimum measurable tilt. $P = \frac{P_{out}}{P_{in}} \approx 3.3\%$, $SNR = 1$.

P_{in}[a](μW)	P_{out}[b](μW)	V[c] (mV)	$\theta_{\min}$(nrad)
210	7	1000	8.29
300	10	800	6.93
400	13	715	6.01
500	17	660	5.37
750	25	560	4.39
1000	33	400	3.8

[a]Sagnac interferometer injected optical power.
[b]Sagnac interferometer output optical power.
[c]Piezo driving voltage (mV).

the input power can decrease the minimum measurable tilt; meanwhile, the linear relationship between the piezoelectric transducer driving voltage and the minimum measurable tilt $\theta_{\min}$ is shown in Fig. 6.

In the aforementioned work, we focus on the SNR and the minimized measurable value in our small-tilt measurement. However, the response curve in dynamics range is also important in quantum measurement, which reflects the capability in the measurement range.[33] The high-order modes induced by the small tilt vs the tilt value are shown in Fig. 7. One can find in Fig. 7 that, with the increase in the tilt, more higher modes, such as TEM_{10}, TEM_{20}, and TEM_{30} modes, will get more weights, and the mode will not pure any more. Therefore, the smaller the tilt, the higher precision the measurement can reach. Considering about our experimental parameters, the waist of the incident TEM_{00} mode is $\omega_0 = 60\,\mu$m, and the wavelength of the probe beam is $\lambda = 1064\,$nm, then $\theta < \lambda/\omega_0 = (1064 \times 10^{-9})/(60 \times 10^{-6}) \approx 0.018$ rad is the condition that the TEM_{10} mode can exist, as is shown by the red curve. The ideal condition of our experiment is shown by the green line, according to Eq. (2). From Fig. 7, the linear measurement range of our system is ± 1.82 mrad for a nonlinearity of 5%, where the green line and the red curve can match well. The condition that this method work is proved to be θ meets $\theta \ll \frac{\lambda}{\omega_0}$, under which almost all the tilt information is contained in the TEM_{10} mode.[15]

We demonstrate the advantage of the combination of the WVA technique and the BHD system compared with the conventional

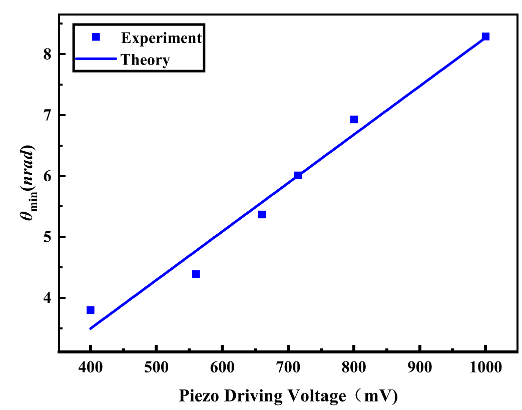

FIG. 6. The minimum measurable tilt vs the piezo driving voltage (the solid line is the theoretical fitting curve).

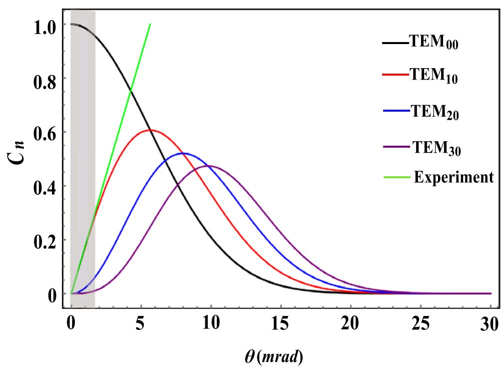

FIG. 7. The high-order modes induced by the small tilt vs the tilt value. C_n is the corresponding probability amplitude.

measurement and the SD system, separately. Then, we implement the WVA + BHD system in an optical small-tilt experiment. The weak-value measurement based on the high-order modes BHD system solves the precision limitation problem that caused by the detector saturation, which is also verified experimentally. Moreover, one can obtain the tilt information of all the photons by detecting only a few photons. Our scheme also explains that the destructive interference process is the essence of the weak-value measurement, from a classic perspective. The present smallest minimum measurable tilt we obtained is 3.8 nrad. However, by purifying the optical mode, improving the conversion efficiency of mode-conversion cavity, and optimizing the interferometer's visibility, we may get bigger inject photon number and, thus, achieve better measurement precision. The WVA + BHD scheme can be expanded to more application scenarios (extremely weak output and wider measurement bandwidth) and can also achieve faster response time and higher detection efficiency (compared with conventional CCD detection). Based on our experimental setup, if we use the spatially squeezed light, higher measurement precision can be obtained. Furthermore, the precision measurement of the optical small tilt can be valuable and useful in some special quantum precision measurements, such as atomic force microscopy and quantum biological measurement, positioning between satellites and so on.

This work was supported by the National Key Research and Development Program of China (Nos. 2021YFC2201802 and 2022YFA1404503), the National Natural Science Foundation of China (NSFC) (Nos. 11874248, 11874249, 62027821, and 12074233), the Natural Science Foundation of Shanxi Province (No. 201801D121007), and the Research Project Supported by the Shanxi Scholarship Council of China (No. 2021-005).

AUTHOR DECLARATIONS

Conflict of Interest

The authors have no conflicts to disclose.

Author Contributions

ChaoXia Zhang: Conceptualization (equal); Data curation (equal); Formal analysis (equal); Investigation (equal); Methodology (equal); Writing – original draft (equal); Writing – review & editing (equal). **Yonglang Lai:** Formal analysis (equal); Investigation (equal); Writing – review & editing (equal). **Rongguo Yang:** Conceptualization (equal); Data curation (equal); Formal analysis (equal); Funding acquisition (equal); Methodology (equal); Project administration (equal); Supervision (equal); Writing – review & editing (equal). **Kui Liu:** Conceptualization (equal); Data curation (equal); Formal analysis (equal); Investigation (equal); Methodology (equal); Supervision (equal). **Jing Zhang:** Formal analysis (equal); Investigation (equal); Supervision (equal); Writing – review & editing (lead). **Hengxin Sun:** Formal analysis (equal); Funding acquisition (equal); Methodology (equal); Writing – review & editing (equal). **Jiangrui Gao:** Conceptualization (equal); Formal analysis (equal); Funding acquisition (lead); Investigation (equal); Methodology (equal); Project administration (lead); Supervision (equal); Writing – review & editing (equal).

DATA AVAILABILITY

The data that support the findings of this study are available from the corresponding author upon reasonable request.

REFERENCES

[1]M. A. Taylor, J. Janousek, V. Daria, J. Knittel, B. Hage, H.-A. Bachor, and W. P. Bowen, Nat. Photonics **7**, 229–233 (2013).
[2]G. Meyer and N. M. Amer, Appl. Phys. Lett. **53**, 1045 (1988).
[3]L. Lugiato, A. Gatti, and E. Brambilla, arXiv:quant-ph/0203046 (2002).
[4]V. Delaubert, N. Treps, C. Fabre, H. A. Bachor, and P. Réfrégier, Europhys. Lett. **81**, 44001 (2008).
[5]M. I. Kolobov, Rev. Mod. Phys. **71**, 1539 (1999).
[6]B. Abbott, R. Abbott, R. Adhikari, P. Ajith, B. Allen, G. Allen, R. Amin, S. Anderson, W. Anderson, M. Arain *et al.*, Rep. Prog. Phys. **72**, 076901 (2009).
[7]L. Scientific, B. P. Abbott, R. Abbott, T. Abbott, F. Acernese, K. Ackley, C. Adams, T. Adams, P. Addesso, R. Adhikari *et al.*, Phys. Rev. Lett. **118**, 221101 (2017).
[8]N. Treps, N. Grosse, W. P. Bowen, C. Fabre, H.-A. Bachor, and P. K. Lam, Science **301**, 940 (2003).
[9]N. Treps, U. Andersen, B. Buchler, P. K. Lam, A. Maître, H.-A. Bachor, and C. Fabre, Phys. Rev. Lett. **88**, 203601 (2002).
[10]H. Sun, K. Liu, Z. Liu, P. Guo, J. Zhang, and J. Gao, Appl. Phys. Lett. **104**, 121908 (2014).
[11]H. Sun, Z. Liu, K. Liu, R. Yang, J. Zhang, and J. Gao, Chin. Phys. Lett. **31**, 084202 (2014).
[12]Z. Li, H. Guo, H. Liu, J. Li, H. Sun, R. Yang, K. Liu, and J. Gao, Adv. Quantum. Technol. **5**, 2200055 (2022).
[13]M. T. Hsu, W. P. Bowen, N. Treps, and P. K. Lam, Phys. Rev. A **72**, 013802 (2005).
[14]M. Lassen, V. Delaubert, J. Janousek, K. Wagner, H.-A. Bachor, P. K. Lam, N. Treps, P. Buchhave, C. Fabre, and C. Harb, Phys. Rev. Lett. **98**, 083602 (2007).
[15]M. T. Hsu, V. Delaubert, P. K. Lam, and W. P. Bowen, J. Opt. B **6**, 495 (2004).
[16]V. Delaubert, N. Treps, M. Lassen, C. C. Harb, C. Fabre, P. K. Lam, and H. A. Bachor, Phys. Rev. A **74**, 053823 (2006).
[17]Y. Aharonov, D. Z. Albert, and L. Vaidman, Phys. Rev. Lett. **60**, 1351 (1988).
[18]Y. Kedem, Phys. Rev. A **85**, 121 (2012).
[19]A. N. Jordan, J. Martínez-Rincón, and J. C. Howell, Phys. Rev. X **4**, 011031 (2014).
[20]D. R. M. Arvidsson-Shukur, N. Y. Halpern, H. V. Lepage, A. A. Lasek, C. H. W. Barnes, and S. Lloyd, Nat. Commun. **11**, 3775 (2020).
[21]G. I. Viza, J. Martínez-Rincón, G. B. Alves, A. N. Jordan, and J. C. Howell, Phys. Rev. A **92**, 032127 (2015).
[22]P. B. Dixon, D. J. Starling, A. N. Jordan, and J. C. Howell, Phys. Rev. Lett. **102**, 173601 (2009).
[23]L. Xu, Z. Liu, A. Datta, G. C. Knee, J. S. Lundeen, Y.-q. Lu, and L. Zhang, Phys. Rev. Lett. **125**, 080501 (2020).

[24] O. S. Magaña-Loaiza, M. Mirhosseini, B. Rodenburg, and R. W. Boyd, Phys. Rev. Lett. **112**, 200401 (2014).
[25] Y. Wang, J. Tang, G. Hu, J. Wang, S. Yu, Z. Zhou, Z. Cheng, J. Xu, S. Fang, Q. Wu *et al.*, Phys. Rev. Lett. **117**, 230801 (2016).
[26] M. Song, J. Steinmetz, Y. Zhang, J. Nauriyal, K. Lyons, A. N. Jordan, and J. Cardenas, Nat. Commun. **12**, 6247 (2021).
[27] C. Krafczyk, A. N. Jordan, M. E. Goggin, and P. G. Kwiat, arXiv:2104.14393 (2021).
[28] K. Lyons, J. Dressel, A. N. Jordan, J. C. Howell, and P. G. Kwiat, Phys. Rev. Lett. **114**, 170801 (2015).
[29] J. Martínez-Rincón, W.-T. Liu, G. I. Viza, and J. C. Howell, Phys. Rev. Lett. **116**, 100803 (2016).
[30] W. Liu, J. Martínez-Rincón, G. I. Viza, and J. C. Howell, Opt. Lett. **42**, 903–906 (2017).
[31] J. C. Howell, D. J. Starling, P. B. Dixon, P. K. Vudyasetu, and A. N. Jordan, Phys. Rev. A **81**, 033813 (2010).
[32] H.-A. Bachor and T. C. Ralph, *A Guide to Experiments in Quantum Optics* (John Wiley & Sons, 2019).
[33] H. Yan, Q. Mao, S. Xie, S. Liu, J. Luo, and H.-c. Yeh, Opt. Lett. **45**, 2792–2795 (2020).